Observation of CEP effect via filamentation in transparent solids

Cheng Gong,[1] Jiaming Jiang,[1] Chuang Li,[1] Liwei Song,[1] Zhinan Zeng,[1,*] Yinghui Zheng,[1] Jing Miao,[1] Xiaochun Ge,[1] Yunpei Deng,[2] Ruxin Li,[1,3] and Zhizhan Xu[1]

[1]*State Key Laboratory of High Field Laser Physics, Shanghai Institute of Optics and Fine Mechanics, Chinese Academy of Sciences, Shanghai 201800, China*

[2]*Fritz-Haber-Institut de Max-Planck-Gesellschaft, Berlin 14195, Germany*

[3]*ruxinli@mail.shcnc.ac.cn*

[*]*zhinan_zeng@mail.siom.ac.cn*

Abstract: We report on the first direct observation of carrier-envelope-phase (CEP) effect during the interaction between few-cycle laser pulses and bulk solid materials. Using 2-cycle mid-infrared laser pulses with stabilized CEP, the CEP effect of tunneling ionization during the laser filamentation in a fused silica is revealed. The phase variation of the accompanying supercontinuum (SC) emission with filamentation at different CEPs of laser pulses can be measured by means of spectral interference technique, as a direct manifestation of the strong field tunneling ionization dynamics in transparent solids.

OCIS codes: (190.4180) Multiphoton processes; (190.4720) Optical nonlinearities of condensed matter; (190.7110) Ultrafast nonlinear optics.

References and links

1. P. M. Paul, E. S. Toma, P. Breger, G. Mullot, F. Augé, Ph. Balcou, H. G. Muller, and P. Agostini, "Observation of a Train of Attosecond Pulses From High Harmonic Generation," Science **292**(5522), 1689–1692 (2001).
2. M. Hentschel, R. Kienberger, Ch. Spielmann, G. A. Reider, N. Milosevic, T. Brabec, P. Corkum, U. Heinzmann, M. Drescher, and F. Krausz, "Attosecond metrology," Nature **414**(6863), 509–513 (2001).
3. Y. Mairesse, A. de Bohan, L. J. Frasinski, H. Merdji, L. C. Dinu, P. Monchicourt, P. Breger, M. Kovačev, R. Taïeb, B. Carré, H. G. Muller, P. Agostini, and P. Salières, "Attosecond Synchronization of High-Harmonic Soft X-rays," Science **302**(5650), 1540–1543 (2003).
4. G. Sansone, E. Benedetti, F. Calegari, C. Vozzi, L. Avaldi, R. Flammini, L. Poletto, P. Villoresi, C. Altucci, R. Velotta, S. Stagira, S. De Silvestri, and M. Nisoli, "Isolated Single-Cycle Attosecond Pulses," Science **314**(5798), 443–446 (2006).
5. E. Goulielmakis, M. Schultze, M. Hofstetter, V. S. Yakovlev, J. Gagnon, M. Uiberacker, A. L. Aquila, E. M. Gullikson, D. T. Attwood, R. Kienberger, F. Krausz, and U. Kleineberg, "Single-Cycle Nonlinear Optics," Science **320**(5883), 1614–1617 (2008).
6. T. Popmintchev, M. C. Chen, P. Arpin, M. M. Murnane, and H. C. Kapteyn, "The attosecond nonlinear optics of bright coherent X-ray generation," Nat. Photonics **4**(12), 822–832 (2010).
7. G. G. Paulus, F. Grasbon, H. Walther, P. Villoresi, M. Nisoli, S. Stagira, E. Priori, and S. De Silvestri, "Absolute-phase phenomena in photoionization with few-cycle laser pulses," Nature **414**(6860), 182–184 (2001).
8. G. G. Paulus, F. Lindner, H. Walther, A. Baltuška, E. Goulielmakis, M. Lezius, and F. Krausz, "Measurement of the phase of few-cycle Laser Pulses," Phys. Rev. Lett. **91**(25), 253004 (2003).
9. W. Quan, Z. Lin, M. Wu, H. Kang, H. Liu, X. Liu, J. Chen, J. Liu, X. T. He, S. G. Chen, H. Xiong, L. Guo, H. Xu, Y. Fu, Y. Cheng, and Z. Z. Xu, "Classical Aspects in Above-Threshold Ionization with a Midinfrared Strong Laser Field," Phys. Rev. Lett. **103**(9), 093001 (2009).
10. M. Gertsvolf, M. Spanner, D. M. Rayner, and P. B. Corkum, "Demonstration of attosecond ionization dynamics inside transparent solids," J. Phys. At. Mol. Opt. Phys. **43**(13), 131002 (2010).
11. A. V. Mitrofanov, A. J. Verhoef, E. E. Serebryannikov, J. Lumeau, L. Glebov, A. M. Zheltikov, and A. Baltuška, "Optical Detection of Attosecond Ionization Induced by a Few-Cycle Laser Field in a Transparent Dielectric Material," Phys. Rev. Lett. **106**(14), 147401 (2011).
12. L. Keldysh, "Ionization in the field of a strong electromagnetic wave," Sov. Phys. JETP **20**, 1037–1314 (1965).
13. A. Couairon, L. Sudrie, M. Franco, B. Prade, and A. Mysyrowicz, "Filamentation and damage in fused silica induced by tightly focused femtosecond laser pulses," Phys. Rev. B **71**(12), 125435 (2005).

#177224 - $15.00 USD Received 1 Oct 2012; revised 20 Dec 2012; accepted 24 Feb 2013; published 2 Oct 2013

14. S. Tzortzakis, L. Sudrie, M. Franco, B. Prade, A. Mysyrowicz, A. Couairon, and L. Bergé, "Self-Guided Propagation of Ultrashort IR Laser Pulses in Fused Silica," Phys. Rev. Lett. **87**(21), 213902 (2001).
15. T. Fuji, N. Ishii, C. Y. Teisset, X. Gu, Th. Metzger, A. Baltuška, N. Forger, D. Kaplan, A. Galvanauskas, and F. Krausz, "Parametric amplification of few-cycle carrier-envelope phase-stable pulses at 2.1 μm," Opt. Lett. **31**(8), 1103–1105 (2006).
16. C. P. Hauri, R. B. Lopez-Martens, C. I. Blaga, K. D. Schultz, J. Cryan, R. Chirla, P. Colosimo, G. Doumy, A. M. March, C. Roedig, E. Sistrunk, J. Tate, J. Wheeler, L. F. Dimauro, and E. P. Power, "Intense self-compressed, self-phase-stabilized few-cycle pulses at 2 microm from an optical filament," Opt. Lett. **32**(7), 868–870 (2007).
17. C. Zhang, P. Wei, Y. Huang, Y. Leng, Y. Zheng, Z. Zeng, R. Li, and Z. Xu, "Tunable phase-stabilized infrared optical parametric amplifier for high-order harmonic generation," Opt. Lett. **34**(18), 2730–2732 (2009).
18. G. Cerullo, A. Baltuška, O. D. Mücke, and C. Vozzi, "Few-optical-cycle light pulses with passive carrier-envelope phase stabilization," Laser Photonics Rev. **5**(3), 323–351 (2011).
19. C. Y. Chien, B. La Fontaine, A. Desparois, Z. Jiang, T. W. Johnston, J. C. Kieffer, H. Pépin, F. Vidal, and H. P. Mercure, "Single-shot chirped-pulse spectral interferometry used to measure the femtosecond ionization dynamics of air," Opt. Lett. **25**(8), 578–580 (2000).
20. J. Liu, R. Li, Z. Xu, and J. Liu, " Sub-picosecond resolved investigation of dynamics of laser driven plasma by broad band chirped-pulse spectral interferometry," AIP Conference **641**, 328–331 (2002).
21. J. P. Geindre, P. Audebert, A. Rousse, F. Falliès, J. C. Gauthier, A. Mysyrowicz, A. D. Santos, G. Hamoniaux, and A. Antonetti, "Frequency-domain interferometer for measuring the phase and amplitude of a femtosecond pulse probing a laser-produced plasma," Opt. Lett. **19**(23), 1997–1999 (1994).
22. Y. H. Chen, S. Varma, I. Alexeev, and H. Milchberg, "Measurement of transient nonlinear refractive index in gases using xenon supercontinuum single-shot spectral interferometry," Opt. Express **15**(12), 7458–7467 (2007).
23. C. Y. Chien, B. La Fontaine, A. Desparois, Z. Jiang, T. W. Johnston, J. C. Kieffer, H. Pépin, F. Vidal, and H. P. Mercure, "Single-shot chirped-pulse spectral interferometry used to measure the femtosecond ionization dynamics of air," Opt. Lett. **25**(8), 578–580 (2000).
24. Á. Börzsönyi, Z. Heiner, A. P. Kovács, M. P. Kalashnikov, and K. Osvay, "Measurement of pressure dependent nonlinear refractive index of inert gases," Opt. Express **18**(25), 25847–25854 (2010).
25. B. E. Schmidt, P. Béjot, M. Giguère, A. D. Shiner, C. Trallero-Herrero, E. Bisson, J. Kasparian, J.-P. Wolf, D. M. Villeneuve, J.-C. Kieffer, P. B. Corkum, and F. Légaré, "Compression of 1.8μm laser pulses to sub two optical cycles with bulk material," Appl. Phys. Lett. **96**(12), 121109 (2010).
26. C. Li, D. Wang, L. Song, J. Liu, P. Liu, C. Xu, Y. Leng, R. Li, and Z. Xu, "Generation of carrier-envelope phase stabilized intense 1.5 cycle pulses at 1.75 μm," Opt. Express **19**(7), 6783–6789 (2011).
27. http://en.wikipedia.org/wiki/Sellmeier_equation.
28. L. Bergé, C. L. Soulez, C. Köhler, and S. Skupin, "Role of the carrier-envelope phase in laser filamentation," Appl. Phys. B **103**(3), 563–570 (2011).
29. S. L. Chin, Femtosecond Laser filamentation, Monography, Springer Series on Atomic, Optical, and Plasma Physics, Vol. 55 (Springer Sci. Business Media, New York 2010).
30. J. Liu, H. Schroeder, S. L. Chin, R. Li, W. Yu, and Z. Xu, "Space-frequency coupling, conical waves, and small-scale filamentation in water," Phys. Rev. A **72**(5), 053817 (2005).
31. L. Sudrie, A. Couairon, M. Franco, B. Lamouroux, B. Prade, S. Tzortzakis, and A. Mysyrowicz, "Femtosecond laser-induced damage and filamentary propagation in Fused silica," Phys. Rev. Lett. **89**(18), 186601 (2002).
32. M. V. Ammosov, N. B. Delone, and V. P. Krainov, "Tunnel ionization of complex atoms and atomic ions in an alternating electromagnetic field," Sov. Phys. JETP **64**, 1191–1194 (1986).
33. M. Kreß, T. Löffler, M. D. Thomson, R. Dörner, H. Gimpel, K. Zrost, T. Ergler, R. Moshammer, U. Morgner, J. Ullrich, and H. G. Roskos, "Determination of the carrier-envelope phase of few cycle laser pulses with terahertz emission spectroscopy," Nat. Phys. **2**(5), 327–331 (2006).
34. G. Cerullo, A. Baltuška, O. D. Mücke, and C. Vozzi, "Few-optical-cycle light pulses with passive carrier-envelope phase stabilization," Laser Photonics Rev. **5**(3), 323–351 (2011).

1. Introduction

Understanding the optical field ionization dynamics is of great importance since the optical field ionization is the initial process during the interaction between femtosecond intense laser pulses and matter in both gas and solid phases. The sub-cycle ionization dynamics in the gas phase has been investigated intensively, e.g. during high order harmonics generation (HHG) [1–6] and high-order above-threshold ionization (ATI) in various gases [7–9]. Very recently, sub-cycle ionization dynamics in transparent solid material has also been observed [10,11]. Gerstvolf et al. showed that the sub-cycle ionization survives in large band gap condensed media [10]. By measuring the differential nonlinear absorption between the major and minor axis of an elliptically polarized laser pulse, and a comparison with theoretical calculations, they confirmed that sub-cycle ionization dynamics are encoded in the ellipticity variation between the incident beam and the transmitted beam. Metrofanis et al. demonstrated a

#177224 - $15.00 USD Received 1 Oct 2012; revised 20 Dec 2012; accepted 24 Feb 2013; published 2 Oct 2013

nonlinear pump-probe scheme to detect the few-cycle laser induced electron density modulation in a fused silica, which enables the detection of sub-cycle ionization dynamics in bulk transparent media [11].

The optical field ionization with an intense laser pulse can be divided into two regimes, multiphoton ionization and tunneling ionization, corresponding to different values of Keldysh parameter γ [12]. The Keldysh parameter is defined as $\gamma = \omega(2m_eI_p)^{1/2}/(eE)$, where ω is the circular frequency of the laser field, I_p is the zero-field ionization energy, E is the electric field strength of the laser pulse, m_e and e are the mass and charge of the electron. γ is effectively the ratio of the laser field frequency to tunneling frequency. As would be expected, a value of $\gamma>>1$ indicates multiphoton ionization, while $\gamma<<1$ implies tunneling ionization is dominating. For 800 nm laser pulse in a fused silica, the laser intensity should be higher than 4.5×10^{13} W/cm^2 to achieve $\gamma = 1$ (here the reduced mass, $m^* = 0.64m_e$ is used [13]), which is much higher than the maximum intensity in the filament [14]. So the tunneling ionization will never be dominant in the filament for 800 nm laser pulse. As the Keldysh parameter is inversely proportional to laser wavelength, if the wavelength of the laser pulse is 1.75 μm, the intensity can be down to 1.0×10^{13} W/cm^2 to achieve $\gamma = 1$. So the tunneling ionization should be considered in the filament for 1.75 μm laser pulse. On the other hand, the tunneling ionization is very sensitive to the instantaneous field strength and therefore the carrier-envelope phase (CEP) becomes a vital parameter for few-cycle laser pulses. Few-cycle ultra-short pulse laser sources with stabilized CEP in the mid-infrared (MIR) spectral region have recently been available due to the progress in optical parametric amplification and pulse compression [15–18]. It is thus possible to investigate the dynamics of tunnel ionization in solids using CEP stabilized laser pulses in MIR wavelength regime.

In this work, the CEP effect of the femtosecond pulse filamentation in transparent solids is investigated by measuring the supercontinuum (SC) emission process. We used fused silica and 2 cycle-long (12 fs), CEP-stabilized laser pulses at 1.75 μm central wavelength in the experiments. By means of spectral interference technique [19–24], the phase of the SC spectra can be retrieved. The CEP effect of the tunneling ionization can thus be inferred by measuring SC emission as a function of laser pulse CEP. This is the first direct observation of CEP effect during the interaction between few-cycle laser pulses and bulk solid materials.

2. Experimental setup and results

The schematic of the experimental setup is shown in Fig. 1(a). The MIR femtosecond laser pulses used in the experiments are produced by a home-made three-stage optical parametric amplifier (OPA) pumped by a commercial Ti: sapphire laser amplifier (Coherent LEGEND-HE-Cryo, 40 fs, 800 nm, 1 kHz, 10 mJ pulse energy). The OPA can offer 40 fs [full width at half maximum (FWHM)] laser pulses with central wavelength of 1.8 μm and a single pulse energy of 1.7 mJ. The laser pulses are focused and coupled into an argon-filled hollow fiber in which the spectrum centered at 1.8 μm is broadened and an accompanying weak supercontinuum in the visible region is generated. Then the dispersion in the mid-infrared region is compensated by a pair of fused silica wedges due to its negative group dispersion (GDD) in the spectral range [25], and CEP-stabilized 0.7 mJ/12 fs laser pulses at 1.75 μm central wavelength are obtained [26].

#177224 - $15.00 USD Received 1 Oct 2012; revised 20 Dec 2012; accepted 24 Feb 2013; published 2 Oct 2013

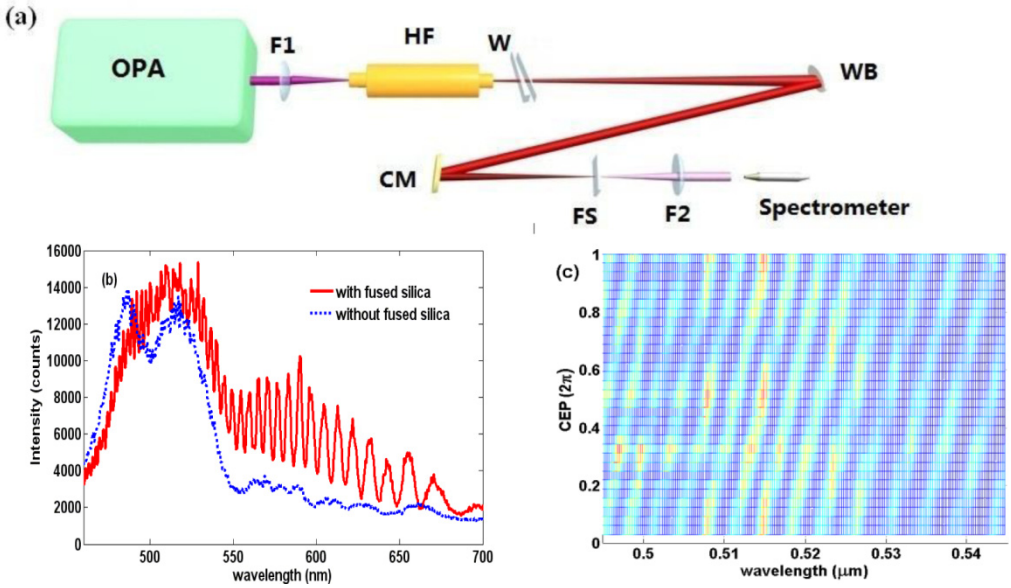

Fig. 1. (a) Experimental setup. The CEP-stabilized laser pulses from the OPA are sent to the argon gas filled hollow fiber (HF) and a dispersion compensator to be compressed down to 12 fs. The CEP of laser pulse is varied by adjusting the thickness of the wedge (W). The laser pulse is then reflected by a white blank (WB) and focused by a concave mirror (CM) into the fused silica (FS) to form the filament, and the transmitted laser spectra are measured by the spectrometer. (b) Measured laser spectra with (solid red line) and without (dash blue line) the supercontinuum generated in the fused silica (FS). (c) The measured spectra with the fused silica as a function of CEP.

In this experiment, only 10 μJ pulse energy is used. The laser pulse is focused by a concave mirror (f = 100 mm) into a fused silica with a thickness of 0.5 mm. The focus spot size is about 30 μm. The fused silica is placed 1 mm after the focus. The supercontinua both from the hollow fiber and generated in the fused silica are collimated by a lens (f = 100 mm) and then measured by a spectrometer (Ocean Optics, USB 2000 +). The signal integral time in the measurement is 100 ms, which means that 100 shots are accumulated to obtain a spectrum. The typical SC measured is shown in red line in Fig. 1(b). For comparison, the SC from the hollow fiber (without the SC generated in the fused silica) is also shown in blue line in Fig. 1(b). The fringes from 480 nm to 700 nm in the spectra (red line) are formed by the interference between the SC from the argon filled hollow fiber and the SC generated by the laser pulse in the fused silica (hereafter referred them as SC1 and SC2 respectively). The fringes are measured as a function of the CEP of the laser pulse (Fig. 1(c)). The CEP is changed by adjusting the wedge thickness, through which the MIR laser pulse and the SC1 propagate. For the MIR laser pulse centered at 1.75 μm, the CEP will shift 2π when the thickness of the wedge changes about 75 μm. For a 12 fs MIR laser pulse with free chirp, the pulse duration will be changed by only 0.07 fs when the thickness of the wedges are changed by 75 μm. So, in our experiment, when the CEP is changed, the intensity of the laser pulse inside the sample will not change too much.

The measured fringes vs CEPs from 0 to 2π in a step of π/16 radian are shown in Fig. 1(c). One can see that the peak position of the interference fringe is shifting continuously as the laser pulse CEP changes, which is owing to the change in the phase of the two SCs. The phase change of the SC can be retrieved, using the spectral interference (SI) technique which has been widely used to study the ultrafast transient refractive change induced by the interaction of the intense laser pulse [22–24]. In the view of SI technique, the SC2 generated in the fused silica during the filamentation acts as a "pump pulse" and the SC1 acts as a

#177224 - $15.00 USD Received 1 Oct 2012; revised 20 Dec 2012; accepted 24 Feb 2013; published 2 Oct 2013

"reference pulse". The resulting interference fringes shift when the phase difference between them is changed. The change of the phase difference can be retrieved from the interferogram from which the CEP effect can be observed (shown in below).

When the thickness of the wedge changes Δz, the phase of SC1, $\varphi_1(\Delta z)$, and the phase of SC2, $\varphi_2(\Delta z)$, can be written as

$$\varphi_1(\Delta z) = \frac{n(\omega) z_0 + (n(\omega) - 1)\Delta z}{c} \cdot \omega + \varphi_{01}, \quad (1)$$

$$\varphi_2(\Delta z) = \frac{n_g z_0 + (n_g - 1)\Delta z}{c} \cdot \omega + f(CEP) + \varphi_{02} \quad (2)$$

where z_0 is the initial thickness of the wedge, ω is the angular frequency of the SC, n(ω) is the refractive index of the fused silica and n_g is the group refractive index of the MIR pulse centered at 1.75 μm in the fused silica. The f(CEP) describes the effect of the CEP, which may be a nonlinear function although the CEP is linearly changed with Δz, φ_{01} and φ_{02} are constant phase which do not change with Δz. The intensity of the 1.75 μm laser pulse is about 2.0×10^{13} W/cm^2. In fused silica, the band gap is 9 eV and the corresponding γ parameter is about 0.71, so tunneling ionization should be taken into account. In SI method, the fringes (e.g. Fig. 1(c)) are Fourier-transformed into the temporal domain to form a main peak with two sidebands. Then one of the sidebands is filtered and Fourier-transformed back to the frequency domain and the phase difference $\varphi_1(\Delta z)$-$\varphi_2(\Delta z)$ can be retrieved.

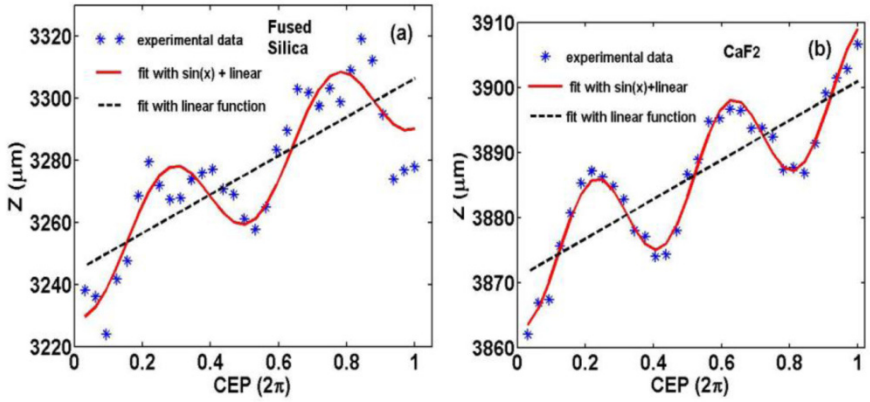

Fig. 2. (a) The results (blue star) obtained by fitting the phase of fringes in Fig. 1(c) with $(n(\omega)-n_g)\omega Z/c$. The black dashed line and red solid curve are the linear fit and the sin(*x*) + linear fit to blue stars, respectively. (b) Similar results obtained with the laser filamentation in CaF_2.

The phase difference, $\Delta\varphi = \varphi_1(\Delta z) - \varphi_2(\Delta z)$, can be written as

$$\Delta\varphi = \frac{(n(\omega) - n_g)\omega}{c} \cdot (z_0 + \Delta z) - f(CEP) + \varphi_{01} - \varphi_{02} \quad (3)$$

Now we can see that the first term in the right of Eq. (3) is the linear function of Δz, which is main contribution of the phase difference. At first, we use the function $(n(\omega)-n_g)\omega Z/c$ to fit the phase difference retrieved from Fig. 1(c). In the calculation, according to Sellmeier equation the refractive index n(λ) can be written as

$$n(\lambda) = \left(1 + \frac{C_1}{1 - C_2^2/\lambda^2} + \frac{C_3}{1 - C_4^2/\lambda^2} + \frac{C_5}{1 - C_6^2/\lambda^2}\right)^{1/2}, \quad (4)$$

#177224 - $15.00 USD Received 1 Oct 2012; revised 20 Dec 2012; accepted 24 Feb 2013; published 2 Oct 2013

where $C_1 = 0.6961663$, $C_2 = 0.0684043$, $C_3 = 0.4079426$, $C_4 = 0.1162414$, $C_5 = 0.8974794$, $C_6 = 9.896161$ [27]. The group refractive index n_g at 1.75 μm is 1.4648. The fitting results (blue stars) are shown in Fig. 2 for different CEPs. Obviously, Z is a nonlinear function of CEP because of the f(CEP) in Eq. (3). As we known, the f(CEP) should be periodic function. Then, we can use a linear function to fit the blue stars because the first and the last two terms of the right side of Eq. (3) are linear. The fitting function is $Z = 9.94\varphi_{CEP} + 3244$ and the result is shown as the black dashed line in Fig. 2(a). With this black dashed line, the linear parts (except for the second term) in Eq. (3) can be removed and the result is shown in Fig. 3(a1), while the relative intensity distribution of the SC is shown in Fig. 3(a2). Furthermore, the relative intensity (blue star) and the nonlinear part of the phase (red cross) at the wavelength of 0.51 μm vs CEP are shown in Fig. 3(b). The blue solid line and the red dashed line are the fitting curves with sine function. One can see that the period of the change in the spectral phase and relative intensity is π (shift of CEP).

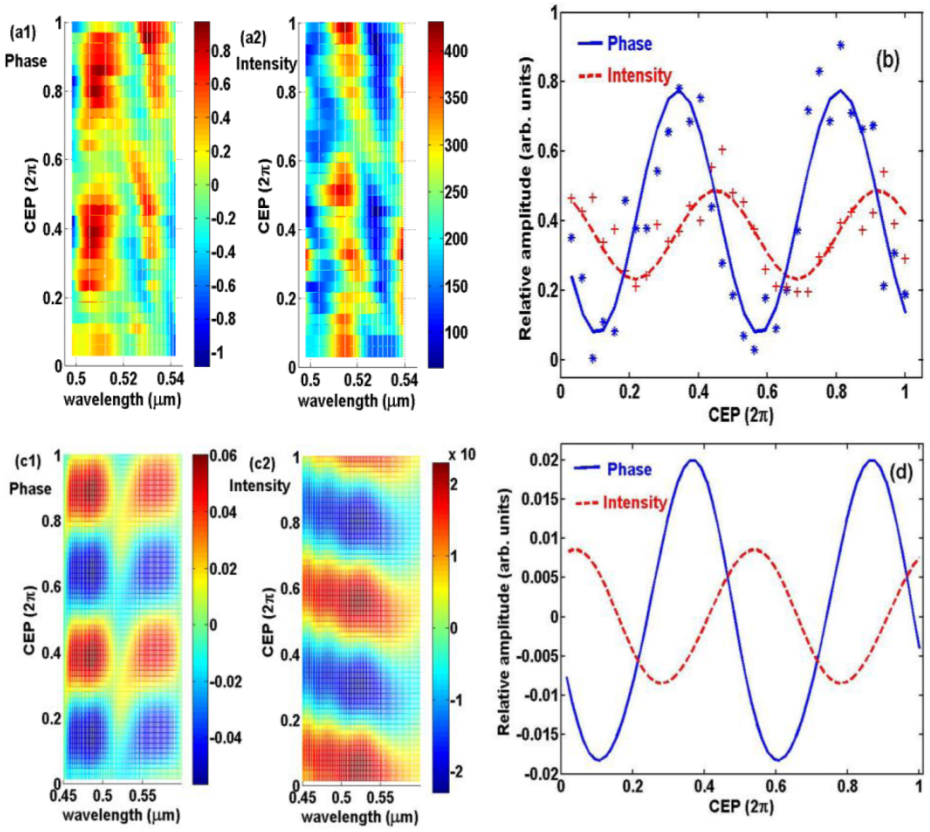

Fig. 3. (a1) The remaining part of the phase retrieved from Fig. 1(c) after removing the linear part. (a2) The relative intensity distributions of the spectra vs CEPs of the laser pulse. (b) The detailed results of the phase (blue solid line) and relative intensity (red dash line) in (a) at 0.51 μm vs CEPs. The phase (c1) and the intensity (c2) of the calculated spectra vs CEPs. (d) The detailed results of (c) at 0.51 μm.

This periodic changing of the spectral phase and intensity is the signal of tunneling ionization. In reference [11], the density of the free carrier is a step function due to tunneling ionization, which leads to the modulation of the probe frequency at $2\omega_0$. The laser pulse duration therein was 25 fs, which is too long to observe the CEP effect. However, in this experiment, the pulse duration is only two cycles, the variation in CEP also leads to the change in free carrier density generated by tunneling ionization.

#177224 - $15.00 USD Received 1 Oct 2012; revised 20 Dec 2012; accepted 24 Feb 2013; published 2 Oct 2013

However, how the SC carry the information of CEP effect of the ionization process? As mentioned above, the CEP will change by 2π for the 1.75 μm laser pulse to propagate every 75 μm in the fused silica. The thickness of the fused silica is 500 μm in the experiment. Then, why the CEP effect can still be measured without being smeared out by the propagating process? In reference [28], the numerical study on the effect of the CEP on the filamentation in noble gas shows that the CEP does not significantly alter the pulse evolution until the pulse duration becomes near-cycle. In our experiment, the propagation of few-cycle laser pulses in fused silica is a complicated process and many mechanisms can lead to the generation of the spectral component at 0.51 μm (hereafter called third harmonic for it is in the regime of third harmonic of the wide input laser spectrum), such as the third harmonic generation (THG), self-phase modulation (SPM) and cross phase modulation (XPM) [29]. To find out the reason, the numerical simulation is done.

3. Numerical simulation and discussion

To understand in more details the underline physical process, a further numerical simulation is done by solving the equation of propagation of axially symmetric electric field can be expressed as [30]

$$\partial_z \tilde{E}(\omega) = ik(\omega)\tilde{E}(\omega) + \frac{i}{2k(\omega)}\nabla_\perp^2 \tilde{E}(\omega)$$
$$-\frac{i\omega n_b n_2}{n(\omega)c}\hat{F}\left[I(t)E(t)\right] + \frac{i}{2\varepsilon_0 n(\omega)\omega c}\frac{e^2}{m}\hat{F}\left[n_e(t)E(t)\right] - \frac{I_p}{2\varepsilon_0 n(\omega)c}\hat{F}\left[\frac{\partial_t n_e(t)}{E(t)}\right] \quad (5)$$

where ω is the angular frequency, n(ω) is the refractive index of different frequency according to Sellmeier equation Eq. (4), k(ω) = n(ω) ω/c, c is the light speed in the vacuum. The n_b and n_2 are linear refractive index and the nonlinear refractive index, respectively. I(t) is the intensity profile of the laser field. $\hat{F}[\cdot]$ represents the Fourier transformation and $\tilde{E}(\omega)$ is Fourier transformation of electric field E(t). The ε_0, e, and m are vacuum permittivity, electron charge and electron mass, respectively. The ionization potential I_p = 9 eV equal to the band gap of SiO_2. The n_e is the density distribution of ionized electron. Because the nonlinear index n_2 at 1.75 μm cannot be found in the previous work, so $n_2 = 3.54 \times 10^{-16}$ cm^2/W for 800 nm laser pulse is used in the simulation [31]. In this simulation, the third term on the right side of Eq. (5) will generate the continuum due to the SPM. The fourth term on the right side of Eq. (5) will generate the harmonics due to quasi-periodic electron density modulation when the tunneling ionization is considered.

The ionized electron is from both the multiphoton ionization and the tunneling ionization (Eq. (6).

$$\frac{\partial n_e}{\partial t} = \sigma_K \left|\hat{E}\right|^{2K} (n_{at} - n_e) + w(E(t))(n_{at} - n_e) - \frac{n_e}{\tau_r} \quad (6)$$

The first term in the right of Eq. (6) denotes the multiphoton ionization [31] in which Ê is the envelope of the electric field and $\sigma_K = 1.3 \times 10^{-55}$ $cm^{10}/W^5/s$ denotes the cross section for multiphoton ionization involving K = 5 photons. The second term in the right of Eq. (6) denotes the tunneling ionization and the ionization rate w(E(t)) is calculated using the Ammosov-Delone-Krainov (ADK) model [32], in which E(t) is the real part of the electric field. The last term in the right of Eq. (6) represents the mechanism of electron recombination and the characteristic time τ_r is 150 fs. The atom intensity n_{at} is 2.1×10^{22} cm^{-3}. The duration of the initial laser pulse is 12 fs and the electric field E(t) will change with the CEP.

#177224 - $15.00 USD Received 1 Oct 2012; revised 20 Dec 2012; accepted 24 Feb 2013; published 2 Oct 2013

When the laser intensity of 1.75×10^{13} W/cm^2 is used in the simulation, the phase and the intensity of the supercontinuum are shown in Fig. 3(c1) and 3(c2). The detailed results for 0.51 μm of different CEPs are shown in Fig. 3(d). The effect of the tunneling ionization can be obviously seen, which agrees with the experimental results shown in Fig. 3(b).

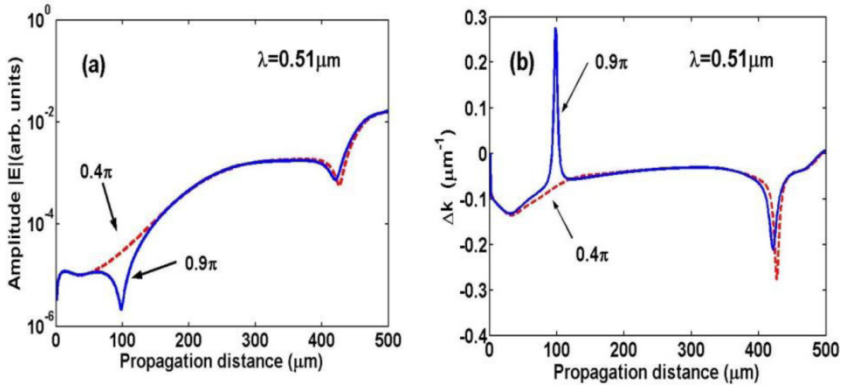

Fig. 4. (a) The amplitude |E| and (b) the wave vector Δk of the third harmonic (0.51μm) as functions of the propagation distance under two different CEP values of laser pulses, the significant difference can be seen at around 100 μm propagation distance.

In order to learn the details of the CEP effect, the intensity and phase change of the third harmonic (0.51 μm) during propagation is shown in Fig. 4(a) and 4(b) respectively. When the propagation distance is less than 100 μm, the third harmonic is very weak because it is generated by the electron density modulation and the electron density due to tunneling ionization is very low. At the same time, the SC generation due to the SPM makes the spectral bandwidth larger and larger. When the propagation distance is about 100 μm, the SC generated by the SPM process extends to the third harmonic (0.51 μm). After that, the intensity of the third harmonic increases rapidly because the SPM is dominant. Around the propagation distance of 100 μm, the intensity change of the third harmonic is quite different under different CEPs, which is shown in Fig. 4(a). This difference leads to a great change of the phase of the third harmonic. As shown in Fig. 4(b), the wave vector $\Delta k = \partial\varphi/\partial z$ of CEP = 0.9π shows a sudden change around 100 μm. After that, the changes of the wave vector of different CEPs are almost the same. Then the effect of the CEP (tunneling ionization) can be kept in the phase of the third harmonic although the electron density of the tunneling ionization is very low and can be detected after the propagation in the 0.5 mm thick fused silica.

We found the demonstrated method is a general technique to detect the CEP effect (the sub-cycle tunneling ionization dynamics) in transparent materials. When the fused silica is replaced by CaF_2 crystal with a thickness of 500 μm, similar results to those shown in Fig. 2(a) are shown in Fig. 2(b). The period of the phase oscillation is the same with that of the fused silica, but the absolute value of the phase change is different. This means the difference in the tunneling ionization process in different materials.

Furthermore, the nonlinear dependence of the SC phase on the CEP has the potential application in the measurement of the CEP value of few cycle laser pulses. Using this spectral interference method, the absolute value of CEP can be determined after a calibration. This method is based on the tunneling ionization process in solids. In comparison with other methods based on the ionization of gaseous atoms or molecules, such as detecting Terahertz-emission [33] and ATI photoelectrons [7], much lower laser intensity is needed.

#177224 - $15.00 USD Received 1 Oct 2012; revised 20 Dec 2012; accepted 24 Feb 2013; published 2 Oct 2013

4. Conclusion

In summary, the CEP effect of tunneling ionization in fused silica during the filamentation process has been demonstrated with the CEP-stabilized few-cycle mid-infrared laser pulses. The phase and the relative intensity of the supercontinuum as functions of the CEP of laser pulses are measured experimentally, in good agreement with the numerical simulation. The method demonstrated in this work is general for investigating the strong field sub-cycle ionization dynamics in the transparent solids.

Acknowledgment

This work is supported by Chinese Ministry of Science and Technology through the 973 program (Grant No. 2011CB808100) and the state key laboratory program, National Natural Science Foundation (Grant Nos. 60921004, 10904157, 60978012, 61078022, 60808008, 11134010), Chinese Academy of Sciences, Shanghai Commission of Science and Technology (Grant Nos. 10QA1407600) and Shanghai Supercomputer Center of China.

#177224 - $15.00 USD Received 1 Oct 2012; revised 20 Dec 2012; accepted 24 Feb 2013; published 2 Oct 2013